Fluidized-Bed Reactor Modeling for Polyethylene Production

FABIANO ANDRÉ NARCISO FERNANDES, LILIANE MARIA FERRARESO LONA

Departamento de Processos Químicos, Faculdade de Engenharia Química, Universidade Estadual de Campinas, 13081-970 Campinas, São Paulo, Brazil

Received 8 March 2000; accepted 10 June 2000

ABSTRACT: Gas-phase technology for polyethylene production has been widely used by industries around the world. A good model for the reactor fluid dynamics is essential to properly set the operating conditions of the fluidized-bed reactor. The fluidized-bed model developed in this work is based on a steady-state model, incorporating interactions between separate bubble, emulsion gas phase, and emulsion solid polymer particles. The model is capable not only of computing temperature and concentration gradients for bubble and emulsion phases, calculating polymer particle mean diameter throughout the bed and polyethylene production rate, but also of pinpointing the appearance of hot spots and polymer meltdown. The model differs from conventional well-mixed fluidized-bed models by assuming that the particles segregate within the bed according to size and weight differences. The model was validated using literature and patent data, presenting good representation of the behavior of the fluidized-bed reactor used in ethylene polymerization. © 2001 John Wiley & Sons, Inc. J Appl Polym Sci 81: 321–332, 2001

Key words: fluidized-bed reactor; polymerization; modeling; simulation; polyethylene

INTRODUCTION

Although fluidized-bed reactor technology for polyethylene production has existed since the mid-1950s, there is still a lack of information concerning the modeling of this reactor. Great advances have been made in basic ethylene polymerization kinetics,[1–3] resistance of the polymer particle to material and heat transfer,[1,4–6] and prediction of polymer particle growth.[7]

In fluidized-bed reactor modeling for polymer production, two main studies have presented a steady-state model for the reactor: Choi and Ray[8] and McAuley et al.,[9] the second study of which is an update of the first study. These two models assume temperature and concentration gradients within the gas bubble phase throughout the bed, assuming the interaction of separate emulsion and bubble phases. McAuley et al.[9] revised the model of Choi and Ray,[8] establishing a maximum stable bubble size and making new assumptions with regard to material and heat transfer mechanisms within the bed. In both works the emulsion phase is considered to behave as a continuous stirred tank reactor, that is, to be fully mixed. This latter assumption is good for small fluidized beds that are violently fluidized and have a height-to-diameter ratio not much different from 1, as demonstrated by Lynch and Wanke.[10] However, for pilot plant and industrial reactors, the height/diameter ratio is often quite large, both to

Correspondence to: L. Lona (liliane@feq.unicamp.br).

Contract grant sponsor: Fundação de Amparo à Pesquisa Estado de São Paulo (FAPESP).

Journal of Applied Polymer Science, Vol. 81, 321–332 (2001)

economize on the use of expensive fluidizing gases and to get the proper contact time to allow polymerization to succeed. The fully mixed approach, therefore, may not be the best approach for modeling this kind of reactor and valuable information about the reactor fluid dynamic behavior can be lost.

Basically all fluidized-bed reactor modeling has been based on the assumption of constant particle size, or at least on an average particle size. This assumption, however, is very distant from the reality inside the fluidized-bed reactor for most polymerization systems. Fluidized-bed reactors used in polymerization reactions usually process solids with a wide distribution of particle sizes. Gas-phase polymerization is a good example of such a particle system. For the polyethylene case, particles can range from 50 μm (catalyst or prepolymer size) up to 4000 μm (full polymer size), and therefore the effect of this broad range of particle sizes, and consequently particle weight, inside the reactor should not be neglected when modeling the fluidized-bed reactor for polyethylene production.[11,12]

The difference in particle size and/or density is a direct reason for segregation, as described in detail by Kunii and Levenspiel,[13] Rowe et al.,[14] Nienow et al.,[15] Geldart et al.,[16] Gibilaro and Rowe,[17] and Sciazko and Bandrowski.[18]

The fluidization of solids with a wide range of particle sizes at a minimum fluidization velocity does not mean that all the particles are suspended in a flowing gas. Gas velocity determines only the equilibrium condition of a partly suspended bed. Moreover, perfect mixing is not directly related to the complete fluidization velocity. A bed may be well fluidized in the sense that all the particles are fully supported by the gas, but may still be segregated in the sense that the local bed composition does not correspond with the overall average, as it was considered in early fluidized-bed models. Segregation is likely to occur when there is a substantial difference in the drag/unit weight between different particles. Particles having a higher drag/unit weight migrate to the surface, whereas those with a low drag/unit weight migrate to the distributor.

In polymers systems in which particles present a broad size distribution, a segregation tendency is found, with larger particles behaving as jetsam and migrating to the bottom of the fluidized bed, whereas smaller particles behave as flotsam and are preferably being concentrated in the top section of the bed.[19] Therefore, prepolymerized particles and fresh catalyst particles will tend to migrate to the upper portions of the reactor, whereas fully grown polymer particles will tend to migrate toward the lower portions of the reactor.

In wide-ranging particle size systems, good mixing of the particles is achieved only under very specific hydrodynamic conditions. The same bubbles now cause segregation when the denser or larger particles tend to fall preferentially through the disturbed region behind each bubble. Even denser or larger particles carried up in the bubble wake from the bottom segregated layer will be shed from the wake and descend rapidly.

Therefore, gas-phase polymerization will present a segregation profile within the fluidized bed. The reactor model for gas-phase polymerization needs to account for particle segregation and its general pathway inside the reactor, to provide a more realistic model for the fluidized-bed polymerization reactor and, consequently, a better prediction of the polymer physicochemical characteristics produced in the reactor.

These facts make the plug flow in the bubble phase perfectly valid for such a regime, but it becomes very doubtful whether the emulsion phase can be modeled as being fully back-mixed. According to Davidson,[20] for pilot plant and industrial reactors, it is much more plausible to assume that there is a plug-flow regime in the emulsion phase as well in the bubble phase.

The research in this current investigation focuses on the modeling of gas-phase polyethylene reactors, assuming that the emulsion phase is in a plug-flow regime. The new model developed in this work also assumes that the polymer particles present a degree of segregation within the fluidized bed, showing size and weight distribution profiles throughout the reactor.

The main goal of this new model is to achieve a more complete understanding of reactor behavior, upgrading the model for fluidized-bed reactors for polyethylene production.

REACTOR FLUID DYNAMICS

The fluidized-bed reactor for polyethylene production comprises three different phases. Reacting and inert gases are fed into the bottom of the reactor through a distributor and splits to form the bubble and emulsion gas phases. The gas in excess for maintaining the minimum fluidization condition passes through the bed as bubbles. Un-

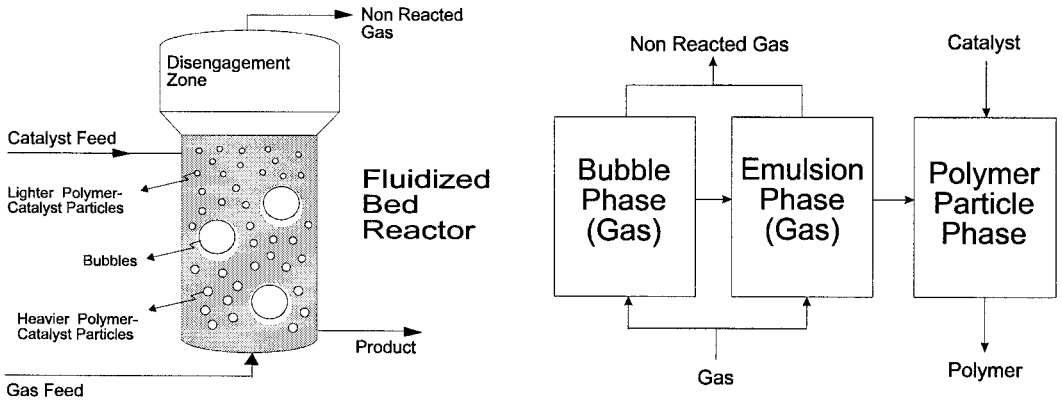

Figure 1 Fluidized-bed polymerization reactor and phases diagram.

reacted gases exiting from the top of the fluidized bed of polymer flow upwardly through a disengaging zone in the upper part of the reactor. The disengaging zone normally is larger in diameter than the polymerization zone, so as to reduce the gas flow velocity and thereby facilitate the settling out of solid particulates. Particles that pass the disengaging zone are separated from the gas phase by means of a cyclone and then are returned to the fluidized bed.

The catalyst is generally fed near the top of the reactor. As the reaction proceeds, polymer is formed in the catalyst surface. During operation of the reactor, new polymer product is continuously formed by the catalyzed polymerization of the gas and product is continuously withdrawn to maintain the fluidized polymer product bed at a substantially constant level.[11,21–24]

Figure 1 shows a schematic view of the fluidized-bed reactor and a diagram of the phases inside the reactor.

The polymer degree of segregation within the fluidized bed can be estimated using eq. (1), for which the mixing index is presented by Wu and Baeyens[19]:

$$M = 1 - 0.0067 d_R^{1.33} [2.27 \mathrm{Ar}^{-0.21} (U - U_{mf})]^{-0.75} \quad (1)$$

where M is the mixing index, d_R is the particle diameter, Ar is the Archimedes number, U is the superficial velocity, and U_{mf} is the minimum fluidizing velocity.

For typical ethylene polymerization systems, the mixing index ranges from 0.4 to 0.5, which can be attributed to poor mixing. Therefore, the emulsion system behaves more like a countercurrent plug-flow reactor than as a well-mixed Continuous Stirred Tank Reactor (CSTR).

MODEL DEVELOPMENT

Model Assumptions

Besides the common assumptions for fluidized-bed reactor models (fluidized bed comprising bubble and emulsion phases, polymerization reaction occurring only in the emulsion phase, emulsion phase at its minimum fluidizing conditions, gas in excess of that required for minimum fluidization passing through the bed as bubbles, bubbles growing only to a maximum stable size and traveling up the reactor in a plug-flow regime), the following additional assumptions were made in the development of the model:

- The emulsion phase also travels up through the bed in a plug-flow regime.
- Polymer particles flow downward and segregate within the bed according to their size and weight. Particles are assumed not to have a constant diameter.
- Ethylene, 1-butene, 1-hexene, hydrogen, and nitrogen are assumed to be present as components of the gas phase. Copolymerization of the ethylene is assumed.
- Considering propagation and chain transfer rates, a two-site kinetic model is assumed.
- Radial concentration and temperature gradients within the bed, resistance to heat, and material transfer between gas and solids and elutriation are assumed to be negligible.

Bubble-Phase Material and Energy Balance

Because bubbles are assumed to be noninteractive spheres, a single bubble is used to infer the behavior of the entire bubble phase.

Table I Reaction Mechanism and Kinetic Parameters

Reaction		Catalytic Site 1	Catalytic Site 2
Propagation [L mol^{-1} s^{-1}]	$R_i(r) + C_k \xrightarrow{kpik} R_k(r+1)$		
		kp_{11} 85	85
		kp_{12} 2	15
		kp_{21} 64	64
		kp_{22} 1.5	6.2
Chain transfer [L mol^{-1} s^{-1}]	$R_i(r) + C_k \xrightarrow{kfmik} P(r) + R_k(1)$		
		kf_{11} 0.0021	0.0021
		kf_{12} 0.006	0.11
		kf_{21} 0.0021	0.001
		kf_{22} 0.006	0.11
	$R_i(r) + H_2 \xrightarrow{kfhi} P(r) + H^*$		
		kfh_1 0.088	0.37
		kfh_2 0.088	0.37
	$R_i(r) \xrightarrow{kfsi} P(r) + H^*$		
		kfs_1 0.0001	0.0001
		kfs_2 0.0001	0.0001

See McAuley et al.[3] $R_i(r)$ is the concentration of live polymers with r length and terminal monomer i; H^* is the concentration of active sites with terminal hydrogen; H_2 is the concentration of hydrogen; and $P(r)$ is the concentration of dead polymers with r length.

Mass transfer between bubble and emulsion phases occurs by diffusion through bubble clouds. Energy transfer between phases occurs as a result of the temperature gradient between the phases and also by the diffusion of gases.

$$\frac{dC_b^i}{dz} = \frac{K_m}{U_b}(C_e^i - C_b^i) \tag{2}$$

$$\frac{dT_b}{dz} = \frac{H_m}{U_b C_b^T c_{pg}^*}(T_b - T_e) \tag{3}$$

where i refers to the different gases fed into the reactor, T refers to total concentration, C_b is the bubble gas concentration, C_e is the emulsion gas concentration, z is the height position, K_m is the mass transfer coefficient, U_b is the bubble velocity, T_b is the temperature in the bubble, T_e is the temperature in the emulsion, H_m is the heat transfer coefficient, and c_{pg}^* is the mass specific heat of the gas.

Emulsion-Phase Material and Energy Balance

To consider the axial temperature and concentration gradients and variations in physical properties within the bed, the material and energy balances of the emulsion phase were developed as differential equations that can be evaluated along the reactor bed height with the bubble phase material and energy balances.

The material balance of the emulsion phase assumes the consumption of gas during the polymerization reaction and the mass transfer between bubble and emulsion phases by diffusion.

$$\frac{dC_e^i}{dz} = \frac{Rp'(1-\varepsilon_{mf})}{\varepsilon_{mf} A U_e} + \frac{K_m(C_b^i - C_e^i)\delta}{(1-\delta)\varepsilon_{mf} U_e} \tag{4}$$

where Rp' is the polymer production rate, ϵ_{mf} is the minimum fluidizing porosity, A is the sectional area of the reactor, U_e is the emulsion velocity, and δ is the bubble volume.

The emulsion phase energy balance consists in energy transfer resulting from the temperature gradient by diffusion of gases, heat of reaction, and heat loss attributed to energy transfer through the reactor wall to the surroundings.

$$\frac{dT_e}{dz} = \frac{[c_{pg}^* K_m(C_b^T - C_e^T) + H_m](T_b - T_e)\delta}{U_e(1-\delta)\varepsilon_{mf} c_{pg}^* C_e^T} - \frac{Rp'(1-\varepsilon_{mf})M_W[-\Delta H - (c_{ps} - c_{pg})(T_e - T_{\text{ref}}) + \pi D U_h(T_e - T_\infty)}{U_e \varepsilon_{mf} c_{pg}^* C_e^T} \tag{5}$$

Table II Correlation Used in the Model

Emulsion-phase volume	$V_e = AH(1 - \delta)$
Bubble-phase volume	$V_b = AH\delta$
Minimum fluidizing velocity[25]	$\frac{1.75}{\varepsilon_{mf}^3}\mathrm{Re}_{mf}^3 + \frac{150(1-\varepsilon_{mf})}{\varepsilon_{mf}^3}\mathrm{Re}_m - \mathrm{Ar} = 0$
	$\mathrm{Re}_{mf} = (29.5^2 + 0.0357\ \mathrm{Ar})^{0.5} - 29.5$
	$\mathrm{Ar} = \frac{d_p^3\rho_g(\rho_s - \rho_g)g}{\mu_g^2}$
Emulsion velocity[26]	$U_e = \frac{U_{mf}}{\varepsilon_{mf}(1-\delta)}$
Bubble velocity[27]	$U_b = U_0 - U_{mf} + 0.711\sqrt{gd_b}$
Bubble fraction[28]	$\delta = \frac{U_0 - U_{mf}}{U_b}$
Mass interchange[28]	$\frac{1}{K_m} = \frac{6}{d_b}\left(\frac{1}{K_{bc}} + \frac{1}{K_{ce}}\right)$
	$K_{bc} = 4.5\frac{U_{mf}}{d_b} + 10.4\left(\frac{D^{0.5}}{d_b^{1.5}}\right)$
	$K_{ce} = 6.78\left(\frac{\varepsilon_{mf}DU_b}{d_b^3}\right)^{0.5}$
Heat interchange[28]	$\frac{1}{H_m} = \frac{6}{d_b}\left(\frac{1}{H_{bc}} + \frac{1}{H_{ce}}\right)$
	$H_{bc} = 4.5\frac{U_{mf}\rho_g c_{pg}}{d_b} + 10.4\left(\frac{k_g\rho_g c_{pg}}{d_b^{2.5}}\right)^{0.5}$
	$H_{ce} = 6.78(\rho_g c_{pg}^* k_g)^{0.5}\left(\frac{\varepsilon_{mf}U_b}{d_b}\right)^{0.5}$
Porosity[29]	$\varepsilon_{mf} = 0586\phi^{-0.72}\frac{1}{\mathrm{Ar}^{0.029}}\left(\frac{\rho_g}{\rho_s}\right)^{0.021}$
Bubble diameter[30]	$d_b = d_{bm} - (d_{bm} - d_{bo})e^{-0.3H/2D}$
	$d_{bm} = 0.652[A(U_0 - U_{mf})]^{0.4}$
	$d_{bo} = 0.00376(U_0 - U_{mf})^2$

V_e is the emulsion volume; H is the reactor height; V_b is the bubble volume; Re is the Reynolds number; d_p is the polymer particle diameter; g is the gravity-acceleration constant; m_g is the gas viscosity; U_0 is the superficial velocity; K_{bc} is the bubble-cloud mass-transfer coefficient; K_{ce} is the cloud-emulsion mass-transfer coefficient; d_b is the bubble diameter; D is the gas-diffusion coefficient; H_{bc} is the bubble-cloud heat-transfer coefficient; H_{ce} is the cloud-emulsion heat-transfer coefficient; k_g is the gas thermal conductivity; and ϕ is a geometrical coefficient.

where M_W is the polymer molar weight, ΔH is the heat of reaction, c_{ps} is the polymer specific heat, c_{pg} is the molar specific heat of the gas, T_{ref} is the reference temperature, D is the reactor diameter, U_h is the overall wall heat transfer coefficient, and T_∞ is the ambient temperature.

The material balance for the polyethylene and catalyst is linked together because the final polymer particle grows on the catalyst particles and their mass cannot be separated. This material balance is given by the mass fraction of catalyst in the polymer (χ), which is a function of the mass of catalyst fed into the reactor, the degree of prepolymerization of the catalyst fed into the reactor (initial value of χ), and the rate of reaction.

$$\frac{d\chi}{dz} = \frac{kpC_e^T\rho_S A(1-\delta)(1-\varepsilon_{mf})M_W}{\chi q_{\mathrm{cat}}} \tag{6}$$

where kp is the propagation rate, ρ_S is the polymer density, and q_{cat} is the catalyst mass flow rate.

The mass fraction of catalyst in the polymer allows not only the calculation of the total poly-

Table III Operational Conditions and Reactor Data Used in the Simulations

Ethylene feed rate	0.50 mol/L
1-Butene feed rate	0.20 mol/L
Hydrogen feed rate	0.05 mol/L
Inert feed rate	0.00 mol/L
Cocatalyst feed rate	0.01 mol/L
Catalyst feed rate	0.20 g/s
Gas feed temperature	316 K
Room temperature	340 K
Catalyst density	2.38 g/cm^3
Catalyst diameter	0.05 mm
Degree of prepolymerization	None
Activation energy	37620 J/mol
ΔH	−3829 J/g
Reactor diameter	396 cm
Reactor height	1097 cm
Bubble diameter	15 cm
δ	0.214
ε_{mf}	0.50
U_{mf}	7.0 cm/s
U_e	34.8 cm/s
U_b	114.0 cm/s

See McAuley et al.,[3,9] Choi and Ray,[8] Hartmann et al.,[11] and Jenkins et al.[22]

mer mass produced in the reactor but also the prediction of particle size and weight along the height of the reactor.

The reaction rate is modeled as a first-order reaction in monomer concentration and in the moment zero of the polymer, substituted here by the χq_{cat} term, which is a good estimate for this moment of the polymer.

$$Rp'(j) = \frac{\sum_{c=1}^{NC}\left\{\left[\sum_{i=1}^{NC} kp_{ci}(j)\alpha^i + \sum_{i=1}^{NC} kf_{ci}(j)\alpha^i\right]C_e^c\right\}\rho_S P_{SA}^j P_{\text{CAT}}^{SA}}{\chi} \quad (7)$$

where j refers to the catalyst site type, kf is the transfer to monomer rate, α is the fraction of terminal monomer i, P_{SA}^j is the fraction of catalyst sites type j in the catalyst, and P_{CAT}^{SA} is the number of mols of active sites per catalyst weight.

The mass fraction of catalyst in the polymer enables the use of more complex reaction mechanisms in the reaction rate model, making possible the use of propagation and termination rates that assume the terminal monomer effect. The reaction mechanism used in this work and its respective kinetics constants are listed in Table I.

The rate expression considers that the gas concentration at the catalyst sites is proportional to the gas concentration in the emulsion phase, because the gases dissolved in the polymer phase are in equilibrium with the gases in the emulsion phase.[4,5] The effect of catalyst deactivation is not included in the model.

Correlations used to predict the bubble fraction in the bed, gas velocities of the bubble and emulsion phases, voidage of the emulsion phase, material and heat transfer coefficients, and maximum stable bubble size are listed in Table II.

Physical parameters and the operational conditions used in the model are listed in Table III.

Model Resolution

Resolution of the model has to follow the physical design of the reactor (Fig. 1).

The flow patterns of the fluidized-bed reactor imply having boarding conditions at the base and the top of the reactor, points $z = 0$ and $z = H$, respectively. The boarding conditions are listed in Table IV.

At the top of the reactor (catalyst-feeding zone; $z = H$), the mass fraction of catalyst in the polymer takes its value from the degree of prepolymerization of the catalyst particles being fed into the reactor. Accumulated polymer production is set to zero because, in the catalyst-feeding zone, the polymer chain has not yet initiated its propagation.

At the base of the reactor (polymer-removal zone and gas-feeding zone; $z = 0$), the gas being fed into the reactor is divided into bubble and emulsion phases, and is kept at the same temperature and concentration as the reactor's feeding conditions.

The boarding conditions cannot be used as an initial value integration to solve the problem of

Table IV Reactor Boarding Conditions

Reactor Position	Boarding Conditions
$z=H$	χ = degree of polymerization
$z=0$	$T_e = T_b = T_0$
$z=0$	$C_e = C_b = C_0$

T_0 is the gas feed temperature and C_0 is the gas concentration at the feeding point.

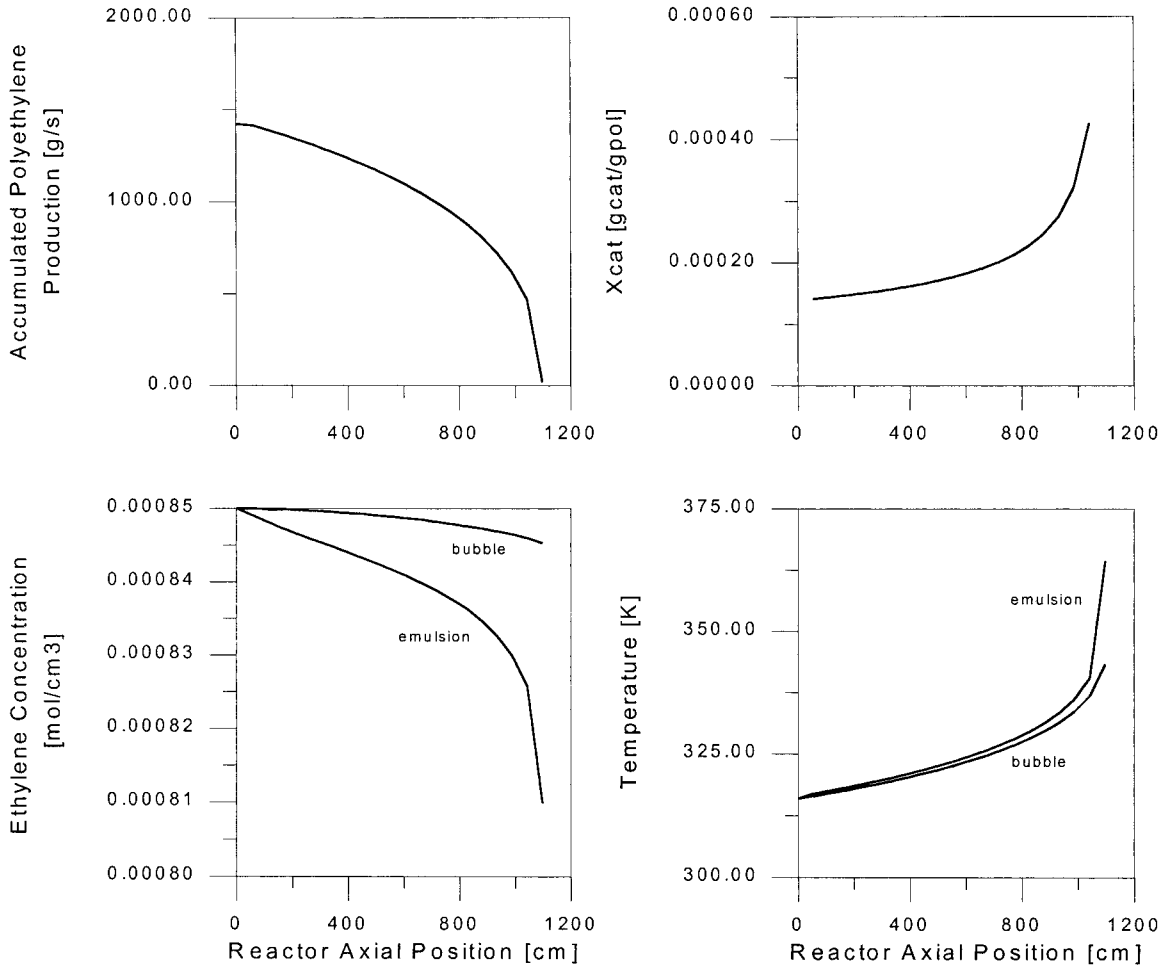

Figure 2 Ethylene concentration, temperature, accumulated polyethylene production, and mass fraction of catalyst in the polymer as a function of the reactor's axial position. Data are from Table III.

reactor behavior. An iterative algorithm needs to be used first to search for an estimate of the values for the mass fraction of catalyst in the polymer and the accumulated polymer production in the reactor's gas-feeding zone ($z = 0$), and then through iterations to solve system behavior until the set of initial values for the reactor's base ($z = 0$) meets the specifications of the boarding conditions of the reactor's catalyst-feeding zone ($z = H$).

MODEL OUTPUTS FOR REACTOR BEHAVIOR

The model developed shows interesting results concerning prediction of temperature and concentration profiles within the reactor, especially in

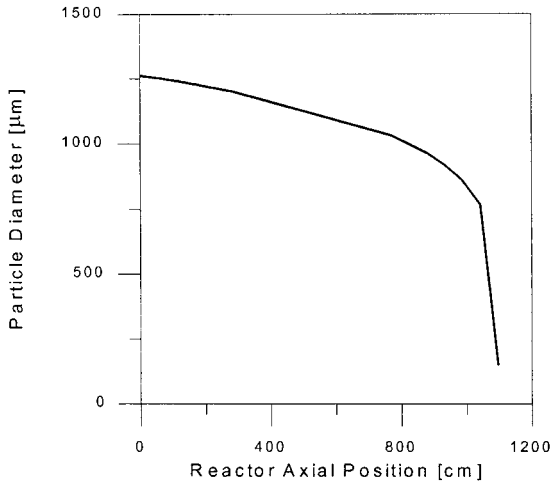

Figure 3 Polymer particle diameter as a function of the reactor's axial position. Data are from Table III.

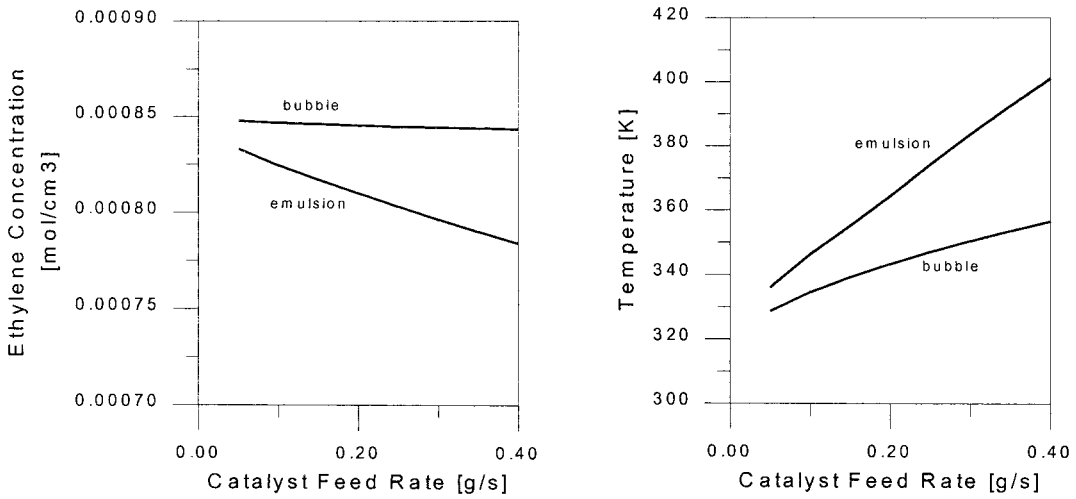

Figure 4 Ethylene concentration and temperature at the top of the reactor (catalyst feeding zone) as a function of the catalyst feed rate. Data are from Table III.

the catalyst-feeding zone, where the reaction rate is higher because of both the higher temperature and the greater influence of the catalyst in the formation and propagation of young polymer particles. A typical result for reactor behavior is shown in Figure 2.

As can be seen, the top portion of the reactor has a more active reaction and, consequently, greater polymer production. This greater production is attributed to the higher activity of the catalyst in the propagation of young polymer particles and to the higher temperature in this region, resulting from reaction heat generation.[31]

The temperature rise in the reactor's top portion is responsible, in many cases, for the appearance of hot spots inside the reactor and the melting and agglomeration of the polymer, which can cause the shutdown of the reactor as a result of clogging of feeding and removal points of the reactor. The greater reaction rate in the reactor's top portion implies a greater consumption of monomer and, therefore, a steeper decrease in the concentration of gases is observed.

If catalyst particles are fed into the reactor at a higher degree of prepolymerization, then a lower difference in temperature and concentration is expected.

It is possible to predict the segregation of the polymer particles within the fluidized-bed height according to its diameter (Fig. 3). Prediction of polymer particle segregation within the fluidized bed is possible only because of the introduction of the mass fraction of catalyst in the polymer into the reactor model.

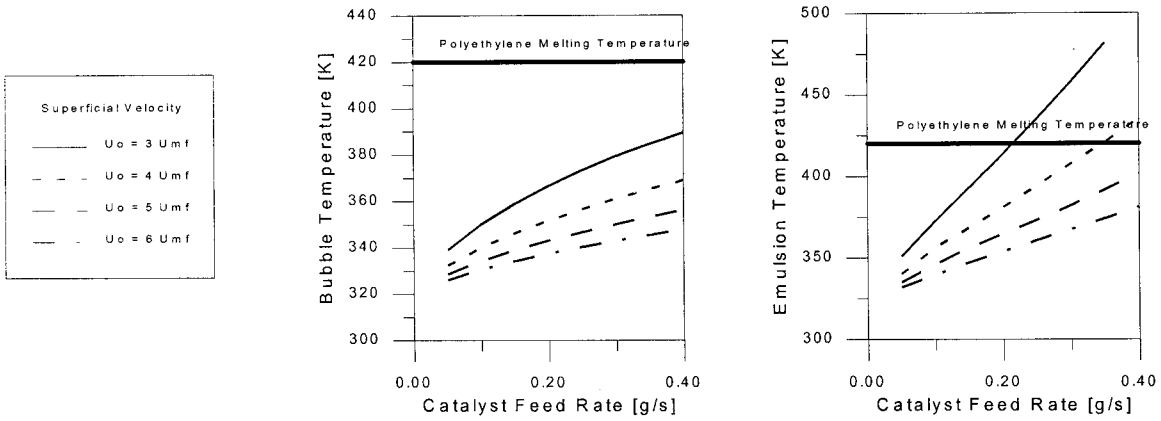

Figure 5 Influence of superficial gas velocity on the temperature of the bubble and emulsion phases.

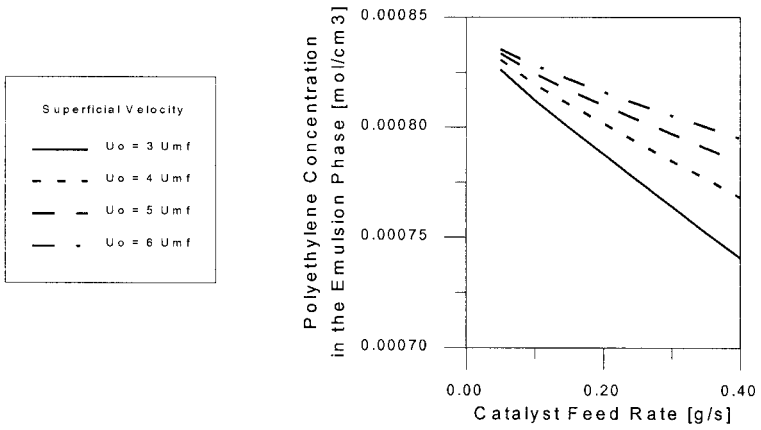

Figure 6 Influence of superficial gas velocity on the ethylene concentration of the gas leaving the reactor.

As can be seen, lighter particles tend to stay at the top of the reactor until they gain mass and fall down into the lower region of the reactor. Full-grown particles reach the bottom of the reactor and are removed.

PARAMETRIC STUDIES

Catalyst Feed

One of the most important operational conditions of the gas-phase process for polyethylene production is the catalyst feed rate, which influences polymer production and physicochemical characteristics.

As the catalyst feed rate rises, the reaction rate also rises, resulting in greater polyethylene production. The temperature of both phases rises as a result of the higher reaction rate. As a consequence, the concentration falls because of the consumption rate, as shown in Figure 4.

Superficial Gas Velocity (U_0)

Superficial gas velocity is a critical operational condition of the system. In industrial reactors, the superficial gas velocity is set at three up to six times the minimum fluidizing velocity, to reduce the risk of polymer melting.[32]

One of the basic functions of the bubbles is to remove the heat produced by the exothermic reaction. When the superficial gas velocity is low, it directly affects the gas residence time in the reactor, which lowers the heat transfer rate between bubbles and emulsion, as seen in Figure 5. The lack of heat removal from the system is a factor of great concern, because for some set of operational conditions the emulsion phase can reach the polymer melting temperature (~ 420

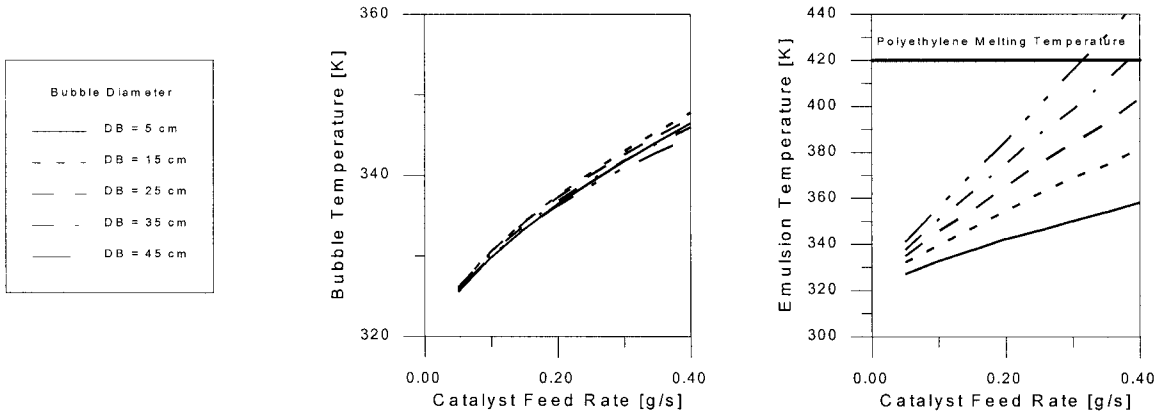

Figure 7 Influence of bubble diameter on the temperature of the bubble and emulsion phases.

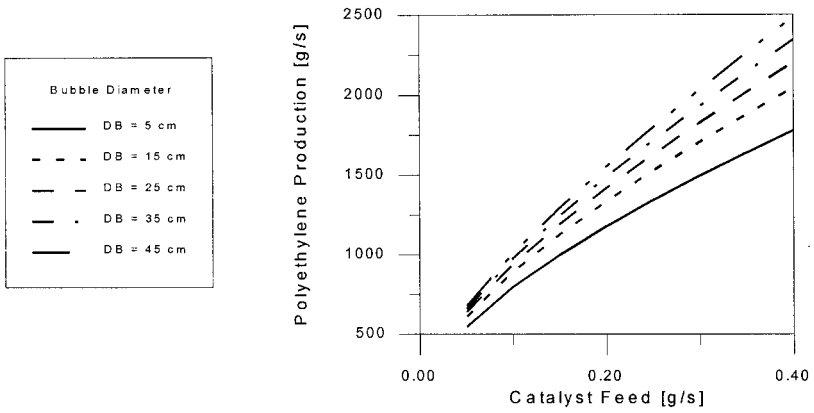

Figure 8 Influence of bubble diameter on polyethylene production.

K). Above five times the minimum fluidizing velocity, the temperature of the emulsion phase does not reach the melting temperature (for catalyst feed rate up to 0.40 g/s).

Higher superficial gas velocities are needed to reduce the risk of polymer melting, even though these higher velocities can lead to greater elutriation of small particles from the bed. In such a case, an efficient system for small particle recovery should be used.

On the other hand, an increase in superficial gas velocity lowers the conversion of a single pass of gas, as can be seen by the concentration of ethylene leaving the reactor (Fig. 6).

Bubble Diameter

Bubble diameter affects the energy and material interchange between bubble and emulsion phases.

As bubble diameters increase, the total interfacial area of the bubbles decreases (the individual interfacial area will increase but the bubbles will decrease in number, and consequently the total interfacial area will also decrease), leading to a lower heat and mass interchange rate between the phases. Emulsion temperature rises as a result of a lower capacity of heat removal. Bubbles above 35 cm in diameter can lead to polymer melting, as shown in Figure 7.

Small bubble diameters have a lower velocity of ascension in the bed compared to that of big bubble diameters. This lower velocity reflects greater volumetric fractions of bubbles in the bed and, therefore, a smaller emulsion phase volume. The lower emulsion phase volume makes the polymer particles in the bed have a lower residence time, reducing the rate of polymerization and the polyethylene production rate (Fig. 8).

Gas Feed Temperature (T_0)

The temperature of the gas fed into the reactor is an operational condition that exerts great influence on the production rate of polyethylene (Fig.

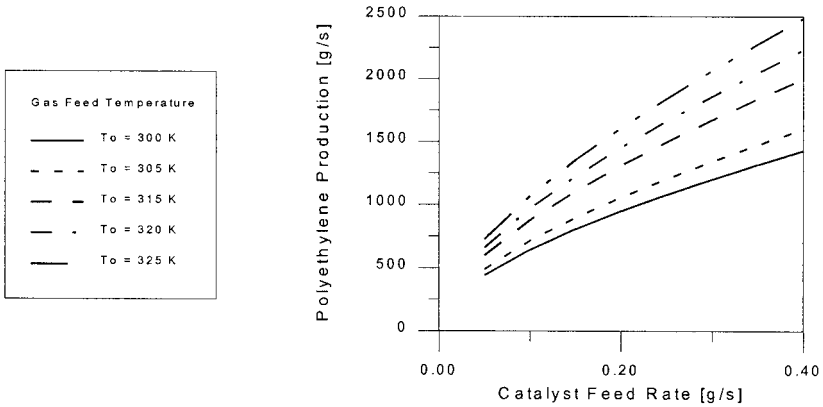

Figure 9 Influence of the gas feed temperature on polyethylene production.

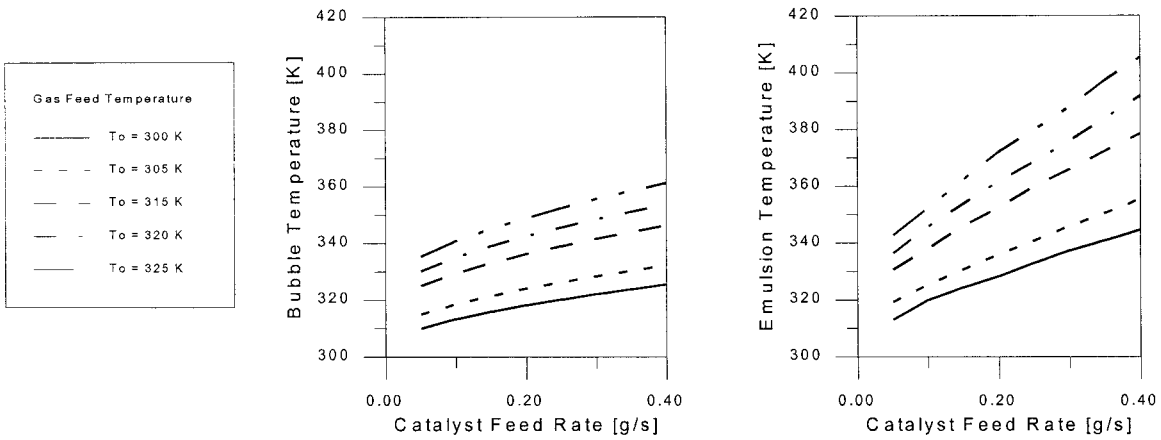

Figure 10 Influence of the gas feed temperature on the temperature of the emulsion and bubble phases at the catalyst feeding zone.

9). As can be seen in Figure 9, a shift of 15 K in the gas feed temperature can increase the production rate of polyethylene by up to 40%. There is also the concern that temperature may reach the polyethylene melting temperature inside the reactor, although temperatures up to 325 K did not present this negative effect (Fig. 10).

CONCLUSIONS

The fluidized-bed reactor model for polyethylene production was reviewed to account for temperature and concentration axial gradients and for the segregation of the polymer particles within the reactor.

The new reactor model developed in this work will allow a more complete understanding of the fluidized-bed reactor for polyethylene production. This model permits the use of complex reaction mechanisms and extends the possibility of simulation to a reactor operating with either a low degree of or no prepolymerization, a case which the models based on the well-mixed emulsion phase theory are unable to predict accurately.

Based on this analysis the use of a plug-flow regime is recommended for the emulsion phase, and the assumption is that the polymer particles segregate inside the reactor.

This model is going to be used to link the reactor model and a model based on characterization of polyethylene physicochemical properties, to perform a complete optimization of the fluidized-bed reactor for the production of polyethylene. Moreover, the model will make possible the optimization of reactor conditions in an attempt to increase the polyethylene production rate and, at the same time, to verify how changes in the operational conditions of the reactor influence the grade of polymer being produced.

The authors acknowledge the financial support of the Fundação de Amparo à Pesquisa do Estado de São Paulo (FAPESP).

REFERENCES

1. Galvan, R.; Tirrel, M. Chem Eng Sci 1986, 41, 2385.
2. deCarvalho, A. B.; Gloor, P. E.; Hamielec, A. E. Polymer 1989, 30, 280.
3. McAuley, K. B.; MacGregor, J. F.; Hamielec, A. E. AIChE J 1990, 36, 837.
4. Floyd, S.; Choi, K. Y.; Taylor, T. W.; Ray, W. H. J Appl Polym Sci 1986a, 32, 2935.
5. Floyd, S.; Choi, K. Y.; Taylor, T. W.; Ray, W. H. J Appl Polym Sci 1986b, 31, 2231.
6. Hutchinson, R. A.; Ray, W. H. J Appl Polym Sci 1987, 34, 657.
7. Hutchinson, R. A.; Chen, C. M.; Ray, W. H. J Appl Polym Sci 1992, 44, 1389.
8. Choi, K. Y.; Ray, W. H. Chem Eng Sci 1985, 40, 2261.
9. McAuley, K. B.; Talbot, J. P.; Harris, T. J. Chem Eng Sci 1994, 49, 2035.
10. Lynch, D. T.; Wanke, S. E. Can J Chem Eng 1991, 69, 332.
11. Hartmann, R.; Dorschner, O.; Gross, H. W. U.S. Pat. 3,931,134, 1976.
12. Wonders, A. G.; Moore, G. E.; Ford, R. R.; Daily, J. R.; Duoley, K. A.; Garela, J. J. U.S. Pat. 5,969,061, 1999.
13. Kunii, D.; Levenspiel, O. Fluidization Engineering; Butterworth-Heineman: London, 1991.

14. Rowe, P. N.; Nienow, A. W.; Agbim, A. J. Trans Inst Chem Eng 1972, 50, 310.
15. Nienow, A. W.; Rowe, P. N.; Chung, Y. L. Powder Technol 1978, 20, 141.
16. Geldart, D.; Baeyens, J.; Pope, J. D.; Van De Wijer, P. Powder Technol 1981, 30, 195.
17. Gibilaro, L. G.; Rowe, P. N. Chem Eng Sci 1974, 29, 1403.
18. Sciazko, M.; Bandrowski, J. Chem Eng J 1995, 60, 89.
19. Wu, S. Y.; Baeyens, J. Powder Technol 1988, 98, 139.
20. Davidson, J. F. AIChE Symp Ser 1992, 87, 1.
21. Roger, D.; Laszlo, H.; Pierre, M. U.S. Pat. 3,922,322, 1975.
22. Jenkins III, J. M.; Jones, R. L.; Jones, T. M. (to Fluidized Bed Reaction Systems) U.S. Pat. 4,543,399, 1985.
23. Platz, G. M. U.S. Pat. 5,143,705, 1992.
24. Dumain, A.; Raufast, C. U.S. Pat. 4,882,400, 1989.
25. Lucas, A.; Arnaldos, J.; Casal, J.; Puigjaner, L. Ind Eng Chem Process Des Dev 1986, 25, 426.
26. Bukul, D. B.; Nasif, N.; Daly, J. G. Chem Eng Sci 1974, 42, 1510.
27. Davidson, J. F.; Harrison, D. Fluidized Particles; Cambridge University Press: New York, 1963.
28. Kunii, D.; Levenspiel, O. Fluidization Engineering; Wiley: New York, 1969.
29. Broadhurst, T. E.; Becker, H. A. AIChE J 1975, 21, 238.
30. Mori, S.; Wen, C. Y. AIChE J 1975, 21, 109.
31. Xie, T.; McAuley, K. B.; James, C. C. H.; Bacon, D. W. Ind Eng Chem Res 1994, 33, 449.
32. Wagner, B. E.; Goeke, G. L.; Karol, F. J. U.S. Pat. 4,303,771, 1985.